

# Simulation of X-Band Signals in a Sand and Dust Storm With Parabolic Wave Equation Method and Two-Ray Model

Mu-Min Chiou and Jean-Fu Kiang

**Abstract**—In this letter, a parabolic wave equation (PWE) method is modified to include the effects of Rayleigh scattering and absorption by dust particles to study microwave signals propagating in a sand and dust storm (SDS). A three-dimensional (3-D) SDS model is proposed, in which the total number density is height-dependent and is circularly symmetric in the horizontal plane. The effects of Earth curvature and ground reflection on microwave wave traversing an SDS are studied by using the PWE method and a two-ray model. A time record of microwave attenuation is also simulated and compared to the measurement data to verify the efficacy of the proposed method.

**Index Terms**—Attenuation, parabolic wave equation (PWE), Rayleigh scattering, sand and dust storm (SDS), two-ray model.

## I. INTRODUCTION

SAND and dust storms (SDSs) may interrupt local-area communications over microwave links [1]–[3], due to signal attenuation and phase fluctuation [2]. Knowledge on the effects of SDSs on microwave propagation helps to predict possible degradation caused by an SDS on ground-based and satellite–ground microwave links [4]. The parameters of SDSs, including particle shape, size distribution, moisture content, and total number density, were studied in [5] and [6], and some relevant works on propagation in SDSs were reviewed [4].

In [3], propagation factor of waves in an SDS was derived in terms of effective material properties. The dependence of attenuation on complex permittivity, frequency, and visibility was also studied by simulations. In [2], formulas of attenuation and phase shift in an SDS were expressed in terms of visibility and frequency, based on the forward Rayleigh scattering amplitude of dust particles.

In [7], a two-dimensional (2-D) SDS model was proposed to simulate the time record of path attenuation. The attenuation thus estimated was found to be in good agreement with the measurement data. However, the SDS properties were assumed to be independent of height, and the effects of ground reflection and Earth curvature were not considered. In practice, the number density of dust particles decreases with height [8]. In addition,

Manuscript received April 20, 2016; accepted May 18, 2016. Date of publication May 19, 2016; date of current version February 27, 2017. This work was supported by the Ministry of Education, Taiwan, under Project 103R3401-1.

The authors are with the Department of Electrical Engineering and the Graduate Institute of Communication Engineering, National Taiwan University, Taipei 10617, Taiwan (e-mail: chumuming@gmail.com; jfkiang@cc.ee.ntu.edu.tw).

Digital Object Identifier 10.1109/LAWP.2016.2570858

the radiation pattern of antennas in typical microwave links, for example, with diameter 1.2 m, mounted at a height of 30 m [9], is significantly affected by the ground at a distance longer than 1.5 km.

In this letter, a practical 3-D SDS is modeled in terms of visibility with horizontal and vertical distributions. The conventional PWE method [10] is modified to include the effects of attenuation and scattering by dust particles. A two-ray model is used to include ground reflection, in which the Earth curvature is considered. Finally, a microwave link in a dust storm in Khartoum, Sudan [9], is simulated to verify the efficacy of the proposed method.

This letter is organized as follows. The visibility distribution and propagation constant in an SDS are presented in Section II. The PWE method and the two-ray model are presented in Section III. The simulations are discussed in Section IV. Finally, the conclusion is drawn in Section V.

## II. VISIBILITY DISTRIBUTION AND PROPAGATION CONSTANT IN SDS

The height profile of visibility was modeled as [5], [8], [11]

$$V_b(z) = V_{b0}(z/z_0)^{0.26} \quad (1)$$

where  $V_{b0}$  is the visibility at a reference height of  $z_0 = 15$  m above ground.

The visibility of an SDS was modeled as a circularly symmetric function in the horizontal plane as [7]

$$V_c(r) = V_a e^{r/r_0} \quad (2)$$

where  $r$  is the distance from the center of the dust storm,  $V_a$  is the minimum visibility at the SDS center ( $r = 0$ ), and  $r_0$  is a reference scale.

By considering both the height profile and the horizontal distribution, a 3-D visibility distribution is proposed as

$$V(r, z) = V_0 e^{r/r_0} (z/z_0)^{0.26} \quad (3)$$

where  $V_0$  is the visibility at  $r = 0$  and  $z = z_0$ .

If Rayleigh scattering is assumed, the specific attenuation constant  $\alpha$  (dB/km) and specific phase shift  $\beta$  (radian/km) were expressed in terms of visibility  $V$  (km) as [2]

$$\alpha = 2.573 \times 10^{-3} \times \text{Im} \left\{ \frac{\epsilon_d - 1}{\epsilon_d + 2} \right\} \frac{f}{V^{1.07}} \quad (4)$$

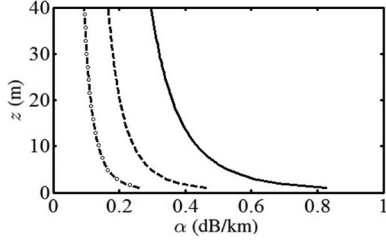


Fig. 1. Height profiles of specific attenuation constant at  $f = 10.5$  GHz,  $V_0 = 3.5$  m,  $r_0 = 9.26$  km,  $z_0 = 15$  m. —:  $r = 0$ , - - -:  $r = 5$  km, - o -:  $r = 10$  km.

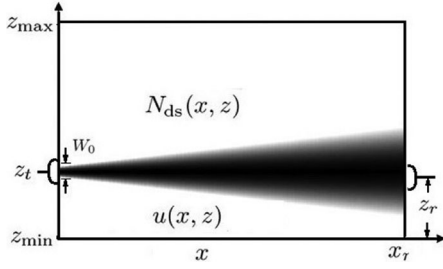


Fig. 2. Schematic of microwave propagation in an SDS.

$$\beta = 1.697 \times 10^{-3} \times \operatorname{Re} \left\{ \frac{\epsilon_d - 1}{\epsilon_d + 2} \right\} \frac{f}{V^{1.07}} \quad (5)$$

where  $f$  (GHz) is the frequency, and  $\epsilon_d = \epsilon'_d - j\epsilon''_d$  is the relative permittivity of dust material. An effective refractivity index in the SDS can then be derived, in terms of  $\alpha$  and  $\beta$ , as

$$n_{\text{ds}} = \frac{\beta}{k_0} \times \frac{1}{1000} \times \frac{\pi}{180} - j \frac{\alpha}{8,686 \times k_0} \quad (6)$$

which is used to characterize the medium when applying the parabolic wave equation (PWE) method.

Fig. 1 shows the height profiles of specific attenuation constant at  $f = 10.5$  GHz, at three different distances from the SDS center, which are obtained by substituting (3) into (4). The values of  $V_0$  and  $r_0$  are derived from [7]. It is observed that at  $r = 0$ , the specific attenuation constant decreases from 0.82 to 0.36 dB/km as the altitude is changed from 1 to 27 m.

### III. MICROWAVE PROPAGATION MODELS

#### A. PWE Method

Fig. 2 shows the schematic of microwave propagation in an SDS, where  $z_t$  is the height of the transmitting antenna,  $x_r$  and  $z_r$  are the range and height, respectively, of the receiving antenna, and  $z_{\min}$  and  $z_{\max}$  are the minimum and the maximum heights, respectively, of the computational domain.

The field distribution in the planar computational domain can be obtained by applying a 2-D PWE method. First, the propagating wave is represented as  $e^{-jk_0 x} u(x, z)$ , where  $u(x, z)$  is called the reduced amplitude function [10]. A vertically polarized wave can be represented with its  $H_y$  component as  $H_y = e^{-jk_0 x} u(x, z)$ .

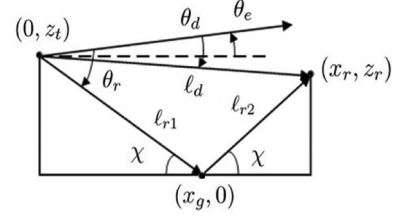


Fig. 3. Schematic of direct and reflected paths above a flat surface.

Next, a Fourier split-step algorithm is applied to march the field in the  $x$ -direction as [10]

$$u(x + \Delta x, z) = e^{-jk_0 m \Delta x / 2} \mathcal{F}^{-1} \left\{ \mathcal{F} \{ u(x, z) \} e^{jp^2 / (2k_0) \Delta x} \right\} \quad (7)$$

where  $\mathcal{F}$  and  $\mathcal{F}^{-1}$  represent the Fourier transform and the inverse Fourier transform, respectively;  $p = k \sin \theta$ ,  $\theta$  is the propagation angle measured from the horizon;  $m = n_{\text{ds}}^2 - 1 + 2z/r_e$  is a modified refractive index, which includes the effect of Earth curvature, and  $r_e$  is the Earth radius. The ground reflection is accounted for by applying a mixed Fourier transform [12], and an absorbing layer is placed on top of  $z_{\max}$  to reduced artificial reflection from the top boundary.

The initial field is approximated with a Gaussian distribution as [13]

$$u(0, z) = \frac{1}{\sqrt{\pi} B} e^{-jk \sin \theta_e z} e^{-(z-z_t)^2 / B^2}$$

where  $B = \sqrt{2 \ln 2} / [k_0 \sin(\theta_0/2)]$ , and  $\theta_0$  is the 3-dB beamwidth.

The attenuation caused by an SDS can be characterized with an attenuation defined as

$$\text{Attenuation} = 20 \times \log_{10} \frac{|u_2(k_0)|}{|u_2(k_{\text{ds}})|} \quad (\text{dB}) \quad (8)$$

where  $k_0$  is the wavenumber in free space.

#### B. Two-Ray Model Over Flat Surface

Fig. 3 shows a two-ray model above a flat surface, where  $\ell_d$  represents the direct path, and a reflected path is composed of line segments  $\ell_{r1}$  and  $\ell_{r2}$ ;  $\theta_e$  is the elevation angle of the antenna with respect to the horizon,  $\theta_d$  and  $\theta_r$  are the angles of the direct path and the reflected path, respectively, with respect to the antenna pointing direction;  $G_a(\theta_d)$  and  $G_a(\theta_r)$  are the antenna gains of the direct and the reflected paths, respectively; and  $x_g$  is the range of the reflection point, and  $\chi = \tan^{-1} [(z_r + z_t)/x_r]$  is the reflection angle.

The total field  $u_2$  at the receiving antenna is the sum of the direct field  $u_d$  and the reflected field  $u_r$  as

$$u_2 = u_d + u_r \quad (9)$$

with

$$u_d = u_0 G_a(\theta_d) \exp \left\{ \int_{\ell_d} -jk_{\text{ds}}(\ell) d\ell \right\} \quad (10)$$

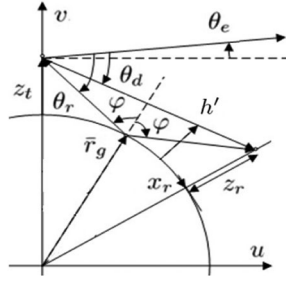


Fig. 4. Schematic of two-ray model above curved surface.

$$u_r = u_0 G_a(\theta_r) \Gamma \exp \left\{ \int_{\ell_{r1}} \ell_{r2} - j k_{ds}(\ell) d\ell \right\} \quad (11)$$

where  $u_0$  is a reference field amplitude,  $k_{ds}$  is the propagation constant in the SDS, and  $\Gamma$  is the Fresnel's reflection coefficient at vertical polarization, with the explicit form of

$$\Gamma = \frac{\sin \chi - \sqrt{(\epsilon_g - \cos^2 \chi)/\epsilon_g^2}}{\sin \chi + \sqrt{(\epsilon_g - \cos^2 \chi)/\epsilon_g^2}} \quad (12)$$

and  $\epsilon_g$  is the permittivity of ground, which is assumed to be  $\epsilon_g = \epsilon_d$ .

### C. Two-Ray Model Above Curved Surface

Fig. 4 shows the schematic of a two-ray model above a curved surface, where the Earth curvature is taken into considerations,  $\varphi$  is the incident angle with respect to the local normal direction at the ground reflection point,  $h'$  is the local height, and  $u$  and  $v$  are coordinates to represent the curved Earth surface. After determining the geometry of two paths, the received field will be calculated by using (9), with the reflection coefficient in (12).

## IV. SIMULATIONS AND DISCUSSIONS

First, we consider a microwave link that passes through the center of an SDS having a visibility distribution  $V(|x - x_{ds}|, z)$ , where  $x_{ds}$  is the  $x$ -coordinate of the SDS center. Similar to the case presented in [9], we choose  $(x_t, z_t) = (0, 30)$  m, and  $(x_r, z_r) = (25 \text{ km}, 27 \text{ m})$ . Based on [7], we choose  $V_0 = 3.5$  m and  $r_0 = 9.26$  km to model the SDS. The center of the SDS is arbitrarily chosen as  $x_{ds} = (x_t + x_r)/2$ .

Fig. 5 shows the height profile of attenuation computed at  $x = 25$  km, by using the two-ray model that takes into account the Earth curvature. Two types of visibility distribution are simulated for comparison. When the visibility depends on height, the attenuation peak is 11.9 dB occurring at a height of 30.2 m. When the visibility is independent of height, the attenuation peak is 11.2 dB occurring at a height of 31.4 m. The height profile of visibility makes the specific attenuation constant a function of height, hence both the direct wave and the reflected wave will be attenuated by different amounts as compared to their counterparts in a height-independent visibility distribution.

If a flat surface is adopted in the model, the attenuation on the direct wave changes almost linearly from 4.5 to 4.2 dB as

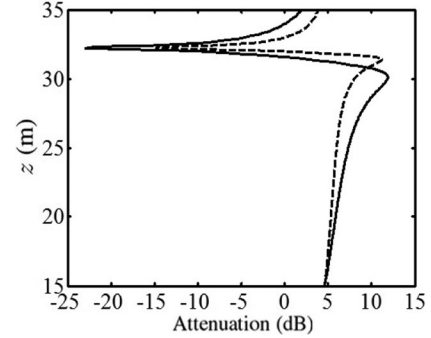


Fig. 5. Height profile of attenuation at  $x = 25$  km by using two-ray model that takes the Earth curvature into account, —:  $V(r, z) = V_0 e^{r/r_0} (z/z_0)^{0.26}$ , ---:  $V(r, z) = V_0 e^{r/r_0}$ .

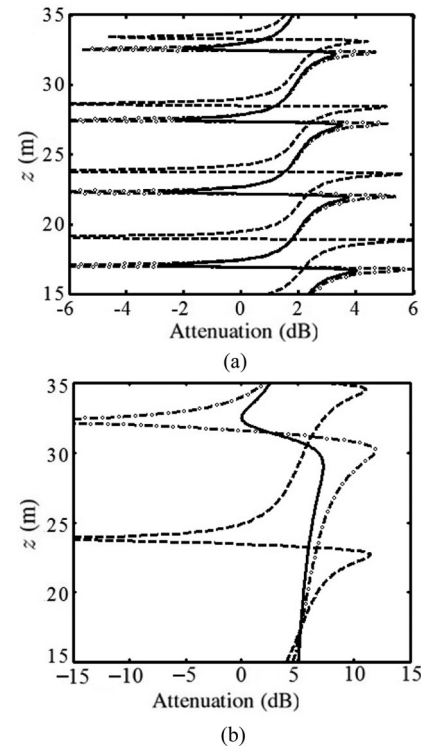


Fig. 6. Height profile of attenuation at (a)  $x = 10$  km and (b)  $x = 25$  km; —: PWE method, ---: two-ray model above flat surface, - o -: two-ray model including Earth curvature;  $\theta_0 = 1.67^\circ$ .

the height of receiving point ( $z_r$ ) changes from 15 to 35 m. If the Earth curvature is included in the model, the attenuation on the direct wave changes almost linearly from 5.2 to 4.5 dB as  $z_r$  changes from 15 to 35 m. The local height of the direct path  $h'$  drops to about 17 m over the range of  $10 < x < 16$  km, leading to more attenuation on the direct wave.

Fig. 6 shows the height profiles of attenuation computed by using the PWE method and the two-ray model, respectively. By using the two-ray model, peaks and nulls appear alternatively with height due to the interference between the direct wave and the ground-reflected wave. The heights of peaks and nulls

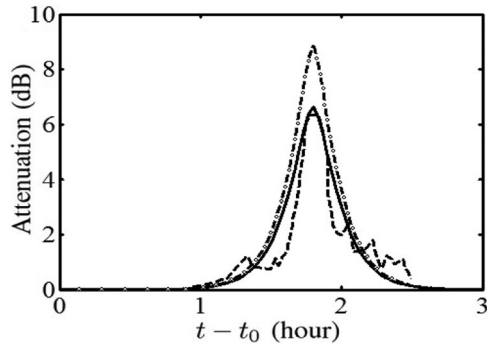


Fig. 7. Time record of attenuation over a microwave link (at  $f = 10.5$  GHz) swept by an SDS, in Khartoum, Sudan, on May 9, 1997. —: PWE method, ---: measurement [9], - · -: two-ray model including Earth curvature.

predicted with two different two-ray models are significantly different.

The heights of peaks and nulls of attenuation computed by using the two-ray model including Earth curvature match well with those obtained by using the PWE method, although the null-to-peak swings of the latter is smaller than those of the former. In the two-ray model, only the two major rays are considered, while the PWE method covers all the wave mechanisms, including diffraction, Earth curvature, and ground reflection [14].

#### A. Comparison to Measurement Data

Finally, the time record of attenuation over a microwave link in Khartoum, swept by an SDS on May 9, 1990 [9], will be simulated. The SDS center was at  $(x_0, y_0)$  at time  $t_0$ , and moved at a constant speed  $v_{ds} = 56$  km/h along a straight line that intersected the microwave link at an angle  $\phi = 45^\circ$ . Thus, the coordinates of the SDS center  $(x_{ds}, y_{ds})$  could be represented as

$$\begin{aligned} x_{ds} &= x_0 + v_{ds}(t - t_0) \cos \phi \\ y_{ds} &= y_0 - v_{ds}(t - t_0) \sin \phi. \end{aligned} \quad (13)$$

By comparing with the record, parameters of the moving SDS track were  $(x_0, y_0) = (-58.5, 71)$  km at  $t_0 = 0$ , and the attenuation peak occurred at  $t = 1.77$  h [9].

About 20 observers were deployed and reported the visibilities to be 2–5 m over a period of 20 min [9]. Based on these data, it was estimated that the observed visibilities 1 m above ground and at radial distances of 9.25 and 37 km from the SDS center were 4.7 and 94 m, respectively [7]. By fitting these data with (3), the SDS distribution parameters were estimated as  $r_0 = 9.263$  km and  $V_0 = 3.5$  m.

In the simulation, a vertically polarized microwave signal at 10.5 GHz is transmitted over the aforementioned link. The transmitting antenna and the receiving antenna are 30 and 27 m, respectively, above the ground. The 3-dB beamwidth of the transmitting antenna is  $1.67^\circ$ . The relative permittivity of dust material is  $5.73 - j0.415$  [5], assuming 30% of water content [9].

Fig. 7 shows the time records of attenuation by measurement [9] and by simulations, respectively, over the microwave link

swept by the SDS. The time record of attenuation predicted with the PWE method agrees reasonably well with the measurement data, and the peak attenuation is also reproduced. The two-ray model including Earth curvature predicts a peak attenuation 2.4 dB higher than the measured value.

## V. CONCLUSION

A PWE method has been modified to include the effects of Rayleigh scattering and absorption by dust particles in an SDS on a microwave link. The effects of Earth curvature, height distribution of SDS properties, and ground reflection are simulated by using the PWE method and the two-ray models, respectively. The two-ray model including Earth curvature predicts a more accurate attenuation profile than its counterpart with a flat surface because the former computes the phase difference between the two paths more accurately than the latter. The spatial distribution and time record of attenuation over a microwave link swept by a moving SDS also simulated. By comparing with the measurement data in the literature, the PWE method can provide a more accurate prediction than the two-ray model.

## REFERENCES

- [1] J. Goldhirsh, "A parameter review and assessment of attenuation and backscatter properties associated with dust storms over desert regions in the frequency range of 1 to 10 GHz," *IEEE Trans. Antennas Propag.*, vol. AP-30, no. 6, pp. 1121–1127, Nov. 1982.
- [2] Q. F. Dong, Y. L. Li, H. Zhang, and M. J. Wang, "Effect of sand and dust storms on microwave propagation," *IEEE Trans. Antennas Propag.*, vol. 61, no. 2, pp. 910–916, Feb. 2013.
- [3] X. Y. Dong, H. Y. Chen, and D. H. Guo, "Microwave and millimeter-wave attenuation in sand and dust storms," *IEEE Antennas Wireless Propag. Lett.*, vol. 10, pp. 469–471, 2011.
- [4] A. Musa, S. O. Bashir, and A. H. Abdalla, "Review and assessment of electromagnetic wave propagation in sand and dust storms at microwave and millimeter wave bands Part I," *Prog. Electromagn. Res. M*, vol. 40, pp. 91–100, Jan. 2014.
- [5] S. Ghobrial and S. M. Sharief, "Microwave attenuation and cross polarization in dust storms," *IEEE Trans. Antennas Propag.*, vol. AP-35, no. 4, pp. 418–425, Apr. 1987.
- [6] A. S. Ahmed, "Role of particle-size distributions on millimetre-wave propagation in sand/dust storms," *IEE Proc., Microw., Antennas Propag.*, vol. 134, no. 1, pp. 55–59, Feb. 1987.
- [7] J. Goldhirsh, "Attenuation and backscatter from a derived two-dimensional duststorm model," *IEEE Trans. Antennas Propag.*, vol. 49, no. 12, pp. 1703–1711, Dec. 2001.
- [8] S. M. Sharif, "Dust storms properties related to microwave signal propagation," *Univ. Khartoum Eng. J.*, vol. 1, no. 1, pp. 1–9, 2011.
- [9] S. I. Ghobrial and J. A. Jervase, "Microwave propagation in dust storms at 10.5 GHz—A case study in Khartoum, Sudan," *IEICE Trans. Commun.*, vol. 80, no. 11, pp. 1722–1727, 1997.
- [10] J. R. Kuttler and G. D. Dockery, "Theoretical description of the parabolic approximation/Fourier split-step method of representing electromagnetic propagation in the troposphere," *Radio Sci.*, vol. 26, no. 2, pp. 381–393, 1991.
- [11] D. A. Gillette, I. H. Blifford, and D. W. Fryrear, "The influence of wind velocity on the size distributions of aerosols generated by the wind erosion of soils," *J. Geophys. Res.*, vol. 79, no. 27, pp. 4068–4075, 1974.
- [12] G. D. Dockery and J. R. Kuttler, "An improved impedance-boundary algorithm for Fourier split-step solutions of the parabolic wave equation," *IEEE Trans. Antennas Propag.*, vol. 44, no. 12, pp. 1592–1599, Dec. 1996.
- [13] I. Sirkova and M. Mikhalev, "Parabolic equation based study of ducting effects on microwave propagation," *Microw. Opt. Technol. Lett.*, vol. 42, no. 5, pp. 390–394, 2004.
- [14] R. Akbarpour and A. R. Webster, "Ray-tracing and parabolic equation methods in the modeling of a tropospheric microwave link," *IEEE Trans. Antennas Propag.*, vol. 53, no. 11, pp. 3785–3791, Nov. 2005.